Quasielastic (e,e') sum rule saturation

C. R. Chinn
Department of Physics and Astronomy, University of Maryland, College Park, Maryland 20742
and Physics Division, Los Alamos National Laboratory, Los Alamos, New Mexico 87545

A. Picklesimer
Physics Division, Los Alamos National Laboratory, Los Alamos, New Mexico 87545

J. W. Van Orden
Continuous Electron Beam Accelerator Facility, Newport News, Virginia 23606
(Received 18 May 1989)

A microscopic Green's function doorway formalism is used to study Coulomb sum rule saturation in inclusive quasielastic electron scattering as a function of momentum transfer. Form factor, kinematical restriction, and final-state interaction effects on the approach to saturation are examined in detail, as are the roles of nonhermiticity, energy dependence, and the analytic behavior of the final-state interactions. The implications of relativistic kinematics and dynamics for the approach to saturation at not-too-high values of the momentum transfer are assessed. Because the pair production of relativistic treatments destroys the asymptotic nature of the nonrelativistic Coulomb sum rule, the degree to which a regime of validity can be expected for this sum rule, and its location, is considered. The breakdown of the sum rule as the momentum transfer increases is also examined. Similar theoretical studies of an analogous nonrelativistic transverse sum in its saturation region are developed as well. Theoretical predictions are compared with the experimental data for ^{40}Ca both directly and using a variety of theoretical prescriptions and limits. Neutron knockout contributions and associated uncertainties due to ambiguity in the free neutron form factors are examined.

I. INTRODUCTION

Unitary properties and especially sum rules serve an important function in providing a forum for theoretical and experimental model-independent comparisons. A longstanding discrepancy exists in quasielastic electron scattering in that the nonrelativistic Coulomb sum rule[1] (NCSR) significantly overestimates the integrated experimental (e,e') longitudinal response. Basically the NCSR states that, as the momentum transfer $|\mathbf{q}|$ increases beyond the point where correlations are significant, the (e,e') energy-integrated longitudinal response $\Sigma_L(|\mathbf{q}|)$ should converge to the number of protons Z in the nucleus. The experimental data is not at present consistent with this limit, in some cases apparently being suppressed by as much as a factor of 2. A number of theoretical alternatives have been offered to explain this inconsistency, including modifications to nucleon size in the nuclear medium,[2-8] quark clustering exchange effects,[9-11] and relativistic dynamical effects.[12-20] Although it remains to be seen whether or not a significant part of this problem is simply associated with the limited experimental data set available, it has certainly become clear over the last few years that there are significant theoretical problems associated with the NCSR itself. The purpose of the studies reported in this paper is to resolve or at least to clarify some of these issues.

The derivation of the NCSR is an unambiguous nonrelativistic construction, depending only on the completeness relation, the nonrelativistic charge operator, and the use of pointlike electromagnetic couplings. In comparing the idealized NCSR with the data a number of complications arise, not the least of which is that the response integral $\Sigma_L(|\mathbf{q}|)$ is not fully accessible experimentally. Currently, basic kinematical and practical restrictions on the experimental data impose the limitation $\omega \lesssim \frac{2}{3}|\mathbf{q}|$. Also, finite-size form-factor corrections must be taken into account before comparing theoretical constructions with experimental data. Nonrelativistic final-state interactions, although often neglected in theoretical analyses, redistribute the quasielastic strength in the $|\mathbf{q}|$-ω plane and so affect both the predicted approach to sum rule saturation and the quasielastic strength hidden in the experimentally inaccessible region. More importantly, the nonrelativistic nature of the derivation of the Coulomb sum rule (CSR) has itself recently been recognized to be a central issue.[18-24] Quasielastic (e,e') and the NCSR are often analyzed within the context of effective one-body models, including the plane-wave impulse approximation (PWIA), the random-phase approximation (RPA),[25-30] the second RPA (SRPA),[31-37] relativistic RPA,[14-20] and most recently the optical model.[12,38,39] Hermitian nonrelativistic models automatically preserve the asymptotic value of Z for the CSR in the relevant limit. However, these models also suggest that sum rule saturation takes place for $|\mathbf{q}| \gtrsim 500$ MeV/c so

that the nonrelativistic expansion of the current operator in powers of $|\mathbf{p}|/m$, where $\mathbf{p}$ is a typical nucleon momentum and m the nucleon mass, is no longer adequate and relativistic considerations are necessary. Even if virtual pair effects are neglected, the corresponding relativistic sum rule converges asymptotically to $Z/2$ rather than to Z due to the fact that the Dirac positive-energy sector spans only half the Hilbert space.[21–23,40] Of course, pair effects cannot be neglected asymptotically and this further obscures the issue. Similarly, the unknown character of the off-shell current operator introduces further uncertainty concerning the CSR.[41] It is apparent that there are a number of theoretical issues which must be examined before a clear understanding of the CSR is obtained.

In seeking a resolution of the apparent disagreement between the quasielastic data and the CSR, it is necessary to reexamine the basic theoretical foundation for the sum rule itself. Rather than introduce additional complexities associated with subhadronic degrees of freedom, it is preferable to first characterize explicit hadronic ingredients and degrees of freedom. Within this context, the theoretical issue is whether or not there exists a region of approximate validity of the NCSR or some extension of it. If there exists such a region, then where in $|\mathbf{q}|$ is this region located and to what extent can the sum rule be expected to be obeyed? It is apparent that long-range correlations, kinematical restrictions, and experimental realities necessitate $|\mathbf{q}| \gtrsim 400$ MeV/c, at least, whereas relativistic, exchange current, and form-factor effects imply some maximum value for $|\mathbf{q}|$. Pair effects together with the relativistic $Z/2$ lmit indicate that the NCSR saturation value of Z is itself in doubt. In this paper the approach to CSR saturation as $|\mathbf{q}|$ increases is studied theoretically. Particular attention is given to the region in $|\mathbf{q}|$ of sum rule stability, its associated CSR prediction, and to the eventual relativistic breakdown of the NCSR as $|\mathbf{q}|$ is further increased.

To numerically examine these aspects of the quasielastic reaction and the CSR it is necessary to simplify the enormous complexity associated with the nuclear many-body problem. In this paper the Green's function doorway approach (GFDA) of Refs. 12 and 38 is employed for this purpose. This formalism permits a relatively clear (nonrelativistic) transcription of the essential features of the many-body quasielastic reaction to an effective one-body problem. Final-state inelastic channels are readily described by means of non-Hermitian potentials, while also preserving the sum rule. The relativistic extension of this formalism parallels that of elastic proton scattering. In short, the GFDA provides an advantageous framework for examining the main physical questions of the many-body quasielastic reaction.

The complement of ingredients needed to fully analyze the sum rule and its saturation can be broadly divided into three categories: (1) nuclear structure, Pauli and long-range correlations, (2) final-state interactions (FSI), relativistic Hilbert-space effects, and relativistic FSI, and (3) the off-shell current operator, exchange currents, and relativistic current corrections. In this paper neither category (1) nor category (3) is addressed. Because our focus is on dynamics we restrict ourselves to larger values of $|\mathbf{q}|$ so that nuclear correlations can be reasonably excluded from our investigations. It is tacitly assumed that the redistribution of quasielastic strength caused by such long-range correlations is negligible at higher $|\mathbf{q}|$ and that the net sum of any redistribution of strength is accounted for and subsumed by the lower portion of the energy integration. The low momentum transfer region has already been investigated by a number of random-phase-approximation calculations.[25–30] The main effects of RPA correlations occur at lower $|\mathbf{q}|$, although nonnegligible effects can also be seen at the higher momenta of interest with respect to CSR saturation.[25,27] Short-range correlations have been shown in a nuclear matter calculation to have an effect at $|\mathbf{q}| \approx 400$ MeV/c.[37,42] RPA extensions to include some 2p-2h contributions have also produced some effects at all values of $|\mathbf{q}|$.[31–37] However, residual hole contributions tend to cancel exchange contributions from the RPA sum, thus leaving self-energy insertions on the particle line or equivalently FSI to dominate the 2p-2h RPA effects.[32]

Relativistic nuclear structure effects have also been investigated by recent relativistic RPA calculations,[14–20] where the isoscalar effective field theory of Ref. 43 is used to determined the p-h residual interactions. Dirac sea correlations originally neglected in relativistic RPA calculations have also led to a linear response for infinite nuclear matter which displays a large suppression (on the order of 30%) of the CSR at all values of $|\mathbf{q}|$.[18] These results are very interesting, but they must be viewed with some caution. For example, it is not yet clear whether these results will persist if a more sophisticated representation of the N-N interaction is used. Also, it has recently been shown[44] that the theory of Ref. 43 is not even qualitatively stable with respect to the loop expansion: results at the one-loop level may be misleading. All of these 1p-1h RPA effects are, of course, in addition to the saturation effects studied here.

Throughout this paper the usual form of the free Dirac current operator is exclusively employed. This choice is motivated on the basis of simplicity and convenience only. It ignores gauge invariance and current conservation constraints as well as the ambiguity in the relativistic off-shell extension of the current operator associated with the Gordon identity. More importantly, the considerable ambiguity associated with the general structure of the off-shell current operator is left unaddressed.[41] This is primarily because the off-shell current operator appropriate for a given circumstance depends not only on hadronic dynamics but also on the detailed substructure and elementary internal currents of the hadrons themselves. The ambiguity in electron scattering analyses which is a direct result of the uncertainty in the off-shell current operator is a subject which has begun to receive increasing attention.[22,41,45] This is clearly an intricate problem which deserves careful attention in its own right. Here, however, all such corrections to the usual current operator are neglected and instead the complementary set of issues in category (2) are focused upon.

The main focus of this paper is thus on the relevance and importance of final-state interactions, and especially relativistic Hilbert space and FSI effects, for understand-

ing CSR saturation and deviations from it. In studying the effects of nonrelativistic FSI on the approach to CSR saturation several models are examined, including microscopic multiple-scattering impulse approximation (IA) optical potentials, a local density approximation (LDA) optical potential, and phenomenological optical potentials. Relativistic FSI are examined through a number of Dirac potentials including IA optical potentials, a phenomenological optical potential, and a real Hartree potential. The roles of non-Hermiticity, energy dependence, and analytic properties of the FSI are examined.

Finally, most of the theoretical issues above are of interest to the integrated transverse response as well, although there happens to be no simple limiting value analogous to Z. Thus, a transverse sum "rule" (TSR) is defined and studied in parallel to our studies of the CSR.[46,47]

Section II briefly reviews the nonrelativistic CSR and relevant aspects of the GFDA to inclusive quasielastic (e,e'). The relativistic extension of the formalism is described and the TSR is defined. Representative results of our studies of sum rule saturation are presented in Secs. III–V. In Sec. III nonrelativistic and relativistic FSI along with relativistic Hilbert-space effects are studied theoretically in the limit of point form factors and in the absence of kinematical restrictions. Section IV then examines finite-size form-factor corrections, neutron contributions, and the numerical significance of kinematical restrictions. Form-factor and kinematical corrections turn out to be important but play only a restricted role in the outcome of our studies, since they can be largely taken into account via specific procedures described in Sec. V. Section V compares our theoretical predictions with the experimental data. Several model-dependent prescriptions have also recently been suggested[21,23,24] for "compensating" the experimental data for a subset of the NCSR violating contributions, specifically the form-factor dependence. Thus, we also compare the results of applying prescriptions to the data and to the theoretical predictions with the appropriate theoretical limiting calculation. A summary of our results and conclusions is given in Sec. VI.

II. FORMAL REVIEW

In the one-photon exchange approximation the quasielastic (e,e') differential cross section is traditionally expressed in terms of the longitudinal (R_L) and transverse (R_T) response functions, so named because they involve the coupling of the nuclear electromagnetic current to longitudinal and transverse virtual photons, respectively. The response functions are defined in terms of the nuclear electromagnetic tensor $W^{\mu\nu}(\mathbf{q},\omega)$ by

$$\begin{aligned} R_L(\mathbf{q},\omega) &= W^{00}(\mathbf{q},\omega) , \\ R_T(\mathbf{q},\omega) &= W^{11}(\mathbf{q},\omega)+W^{22}(\mathbf{q},\omega) , \end{aligned} \tag{1}$$

where the nuclear tensor is given in terms of matrix elements of the hadronic current operator by

$$W^{\mu\nu}(\mathbf{q},\omega)=\overline{\sum_i}\sum\!\!\!\!\!\!\int_f \langle i|\hat{J}^{\mu}(q)^{\dagger}|f\rangle\delta(E_i+\omega-E_f) \times\langle f|\hat{J}^{\nu}(q)|i\rangle . \tag{2}$$

Here $|i\rangle$ is the full initial state of the A-body nucleus, $|f\rangle$ denotes a particular final state of the full hadronic many-body assembly, $\hat{J}^{\mu}(q)$ is the nuclear electromagnetic current operator, and $\overline{\sum}$ denotes an average.

The spectral sum in (2) runs over all possible final states $|f\rangle$ of the interacting many-body assembly so that an exact evaluation of (2) lies well beyond current analytical methods. The treatment of complex reaction channels corresponding to the knockout of many nucleons or clusters of nucleons is perhaps the most conceptually difficult problem involved in applying practical approximations to (2).[12,38] Because of this, and because this paper mainly concerns itself with the behavior of quasielastic scattering at larger momentum and thus energy transfer, it is convenient to suppress the discrete final-state contributions to (2) which occur at very low ω. This allows one to focus on the scattering spectrum in (2) and leads to a continuum doorway approach to the quasielastic contributions of this spectrum.[12] Of course, in examining the summed quasielastic strength it is then necessary, in principle, to appropriately incorporate the discrete state strength by hand.

Suppressing the discrete state contributions to (2), the nuclear response tensor $W^{\mu\mu}$ can be expressed in terms of the virtual Compton amplitude $T^{\mu\nu}$, which describes the elastic forward scattering of virtual photons,

$$W^{\mu\mu}(\mathbf{q},\omega)=\frac{-1}{\pi}\mathrm{Im}T^{\mu\mu}(\mathbf{q},\omega) , \tag{3}$$

where

$$T^{\mu\mu}(\mathbf{q},\omega)=\overline{\sum_i}\langle i|\hat{J}^{\mu}(q)^{\dagger}\hat{G}(\omega+E_i)\hat{J}^{\mu}(q)|i\rangle . \tag{4}$$

Here, $\hat{G}$ is the full many-body propagator for the final nuclear system.

Especially to the extent that bound-state independent-particle motion and a one-body current operator represent reasonable lowest-order starting points, a first-order one-body approximation to (2)–(4) can be reliably formulated[12] resulting in the replacement of $\mathrm{Im}\hat{G}$ by the appropriate one-body ejectile-nucleus optical theory Green's function in each of the single-nucleon knockout channels α_1:

$$\begin{aligned} \mathrm{Im}\hat{G} &= \mathrm{Im}\sum\!\!\!\!\!\!\int_f |f\rangle\langle f|\hat{G}|f\rangle\langle f| \\ &\simeq \mathrm{Im}\sum_{\alpha_i}|\phi_{\alpha_i}\rangle\langle\phi_{\alpha_i}|\hat{G}|\phi_{\alpha_i}\rangle\langle\phi_{\alpha_i}| \\ &= \mathrm{Im}\sum_{\alpha_i}P_{\alpha_i}\hat{G}P_{\alpha_i}=\mathrm{Im}\sum_{\alpha_i}P_{\alpha_i}G_{\mathrm{opt}}^{\alpha_i}P_{\alpha_i} \\ &\simeq \mathrm{Im}\sum_{\alpha_i}P_{\alpha_i}G_{\mathrm{opt}}P_{\alpha_i} . \end{aligned} \tag{5}$$

In (5), $|\phi_{\alpha_i}\rangle$ denotes a plane wave coupled to the bound residual-nuclear state of the one-body knockout channel α_i, P_{α_i} the projector onto the corresponding one-nucleon

knockout space, and $\hat{G}^{\alpha_i}_{\rm opt}$ the optical Green's function for this channel.[48] In reaching the final equation of (5) differences among the α_i-channel optical potentials are neglected and the optical potential for elastic scattering from the target is employed. The formalism associated with all of this is detailed in Ref. 12 and will not be repeated here. We only note that this approach represents a continuum doorway approximation in which the doorway space is the space spanned by the set of one-body knockout subspaces. More complicated final states are properly incorporated through the non-Hermitian optical potential which redistributes flux and allows it to enter and leave the doorway space. Thus the GFDA which we employ consists of (1)–(4) and

$$\mathrm{Im}T^{\mu\mu} \simeq \mathrm{Im}\overline{\sum_i}\sum_{\alpha_i}\langle i|\hat{J}^{\mu}(q)^{\dagger}P_{\alpha_i}G^{\alpha_i}_{\rm opt}P_{\alpha_i}\hat{J}^{\mu}(q)|i\rangle \tag{6a}$$

$$= \mathrm{Im}\overline{\sum_i}\sum_{\alpha_i}\langle i|\hat{J}^{\mu}(q)^{\dagger}|\phi_{\alpha_i}\rangle G^{\alpha_i}_{\rm opt}\langle\phi_{\alpha_i}|\hat{J}^{\mu}(q)|i\rangle \ . \tag{6b}$$

The actual computations reported in this paper are performed assuming, for simplicity, a single Slater determinant target wave function and correspondingly simple one-body knockout states. Accordingly, (6) becomes

$$\mathrm{Im}T^{\mu\mu} \simeq \mathrm{Im}\sum_{i_{(1)}}\langle i_{(1)}|\hat{J}^{\mu}_{(1)}(q)^{\dagger}G_{\rm opt}(E_i+\omega)\hat{J}^{\mu}_{(1)}(q)|i_{(1)}\rangle \ . \tag{6c}$$

Thus the $|i_{(1)}\rangle$ denote the single-particle states occupied in the target. The influence of more sophisticated nuclear structure models on quasielastic scattering and the CSR have already been studied in detail.[14–20,25–37] At the momentum transfers relevant to this paper, it is assumed that the dynamical issues of interest may be studied independently of any residual complications from more realistic nuclear structure models. A more detailed derivation and discussion of (6), its relativistic extension, and the computational methods used in its evaluation can be found in Ref. 12. Here it is noted that the relativistic Dirac dynamical extension of (6) is obtained by replacing the adjoint and adjoint states in (6) by their corresponding Dirac adjoints and by replacing the nonrelativistic $G_{\rm opt}$ by Dirac optical-model Green's functions derived from elastic proton scattering analyses.[12,49]

An important formal property of the (nonrelativistic) one-body GFDA outlined above is the fact that the spectral sum in (2) reduces to a one-body completeness relation which parallels the many-body completeness relation satisfied by the intermediate states in the full treatment of (2). This property is crucial because the completeness relation is at the heart of the derivation of the NCSR. The analog of (2) satisfied by (6a) and (6b) is[12]

$$W^{\mu\mu} \simeq \overline{\sum_i}\sum_{\alpha_i}\langle i|\hat{J}^{\mu}(q)^{\dagger}P_{\alpha_i}\left[\sum_s|\psi_s\rangle\delta(E_i+\omega-E_s)\langle\psi_s|\right]P_{\alpha_i}\hat{J}^{\mu}(q)|i\rangle$$
$$= \overline{\sum_i}\sum_{\alpha_i}\langle i|\hat{J}^{\mu}(q)^{\dagger}|\phi_{\alpha_i}\rangle\left[\sum_s\langle\phi_{\alpha_i}|\psi_s\rangle\delta(E_i+\omega-E_s)\langle\psi_s|\phi_{\alpha_i}\rangle\right]\langle\phi_{\alpha_i}|\hat{J}^{\mu}(q)|i\rangle \ , \tag{7}$$

where the spectral sum runs over the full set of many-body scattering states $|\psi_s\rangle$. The continuum doorway nature of (6) also becomes clear in (7). For example, let $|\psi_s\rangle$ denote a particular inelastic scattering state of arbitrary complexity, say a five-nucleon knockout state. In the vicinity of the residual nucleus, $|\psi_s\rangle$ consists of a complicated superposition of components of many asymptotic characters, including P_{α_i}-space components. It is these latter components of $|\psi_s\rangle$ which are coupled directly to the ground state through the current operator in (6) and (7). Thus quasielastic strength is fed into $|\psi_s\rangle$, and into other open scattering channels of arbitrary complexity, through the continuum doorway provided by the set of P_{α_i}. To the extent that the current operator has the (approximate) one-body property that it only couples $|i\rangle$ to scattering states which lie in the P_{α_i} spaces anyway, (7), and thus (6), essentially reproduce the actual distribution of the quasielastic strength in the $\mathbf{q}$-ω plane.[50] This same assumption also allows[50] us to dispense with the explicit appearance of the P_{α_i} projectors in (7). The spectral sum in (7), and so in (6), then reproduces the many-body completeness relation (assuming an appropriate ancillary treatment of the discrete states) and a crucial ingredient to the NCSR is maintained. From the formal perspective of (6a) and (6b) this is completely satisfactory.

However, for the actual computations using (6c), which involve further approximations certain to compromise the formal analytical properties of (6a) and (6b), a more pragmatic view must be taken. As described shortly, calculations performed on the basis of (6c) can be tailored to take advantage of (7) and to maintain the essential completeness property to good approximation. Plane-wave and Hermitian potential models of the quasielastic process limit the space of the final scattering states, thus ensuring a completeness relation within the model space. These approaches automatically maintain the NCSR limit, but do so at the expense of not providing a conceptually clear, realistic physical description of the complicated inelastic final states of the system.

The mathematical CSR integral $\Sigma_L(|\mathbf{q}|)$ is defined by

$$\Sigma_L(|\mathbf{q}|) = \int_{0^+}^{\infty} R_L(\mathbf{q},\omega)d\omega \ , \tag{8}$$

where $0^+ = \lim \epsilon \to 0^+$ excludes the elastic peak. Using (1) and (2) in (8), and assuming a nondegenerate ground

state $|i\rangle$ leads to

$$\Sigma_L(|\mathbf{q}|)=\langle i|\hat{J}^0(q)^\dagger\hat{J}^0(q)|i\rangle-|\langle i|\hat{J}^0(q)|i\rangle|^2 \tag{9}$$

and it is from (9) that the NCSR

$$\Sigma_L(|\mathbf{q}|)=Z+C(|\mathbf{q}|) \tag{10}$$

is derived. Here, $C(|\mathbf{q}|)$ is the usual two-particle correlation function defined in a nonrelativistic framework by

$$C(|\mathbf{q}|)=\langle i|\int d^3xd^3x'e^{i\mathbf{q}\cdot(\mathbf{x}-\mathbf{x}')}\phi^\dagger(\mathbf{x})\phi^\dagger(\mathbf{x}')\hat{e}_x\hat{e}_{x'}\phi(\mathbf{x}')\phi(\mathbf{x})|i\rangle-Z^2|f_{\rm ch}(\mathbf{q})|^2\ , \tag{11}$$

where $\hat{e}_x$ is the charge operator, $f_{\rm ch}(\mathbf{q})$ is the point proton charge form factor of the nucleus, and $\phi(\mathbf{x})$ is the usual field operator. By way of comparison, the corresponding result for the optical theory Green's function approach which follows from (7) and (8) is

$$\Sigma_L^{\rm opt}(|\mathbf{q}|)=\sum_{\alpha_i}\langle i|\hat{J}^0(q)^\dagger P_{\alpha_i}SP_{\alpha_i}\hat{J}^0(q)|i\rangle\ , \tag{12}$$

where S denotes the projector onto the space spanned by the A-body scattering states. To recover (9) some approximations are necessary. Noting that S contains no $|i\rangle$ bound-state component, assume $P_{\alpha_i}SP_{\alpha_j}\simeq 0$, for $i\neq j$, thus leading to

$$\sum_{\alpha_i}P_{\alpha_i}SP_{\alpha_j}\simeq\sum_{\alpha_i}P_{\alpha_i}S\sum_{\alpha_j}P_{\alpha_j}=\Pi S\Pi\ ,$$

where Π is the projector onto the Hilbert space spanned by the set of P_{α_j}. Since to lowest order $\hat{J}^0(q)$ has been taken to be a one-body operator, $S\Pi\hat{J}^0(q)\simeq S\hat{J}^0(q)$ and by including the discrete state contribution omitted in (2), (9) is recovered. These approximations are discussed in detail in Ref. 12. To the extent that they are reliable, the optical theory GFDA provides an advantageous one-body framework within which to study the dynamics of sum rule saturation as well as the departures from it which arise from physical effects which compromise the applicability of the NCSR.

One such physical effect is due to the (ultrarelativistic) kinematic restriction on (e,e') scattering, namely, $\omega\leq|\mathbf{q}|$. Because of this physical restriction, experimental access to the response functions through electron scattering is limited and an integral of the physical quasielastic strength,

$$S_L(|\mathbf{q}|)=\int_{0^+}^{|\mathbf{q}|}R_L(\mathbf{q},\omega)d\omega\ , \tag{13}$$

is more directly related to experiment than is $\Sigma_L(|\mathbf{q}|)$. In addition, experimental practicalities have so far resulted in the more stringent restriction $\omega\lesssim\frac{2}{3}|\mathbf{q}|$. Because FSI redistribute the quasielastic strength in $|\mathbf{q}|$-ω, the strength which is accessible to experiment, and hence the degree of actual saturation of the NCSR which should be observed, is dependent on the dynamics. The practical implications and ambiguity introduced by these restrictions is studied in the following sections, along with nonrelativistic and relativistic FSI effects and finite form-factor effects. The validity of the NCSR depends on (1) nonrelativistic dynamics, (2) use of the free nonrelativistic current operator, (3) point form factors, (4) neglect of any effects from the kinematical restrictions, and (5) negligible impact of differing dynamics on (4). The basic aim of this paper is to study the behavior of CSR saturation as these assumptions are relaxed. This is done within the context of the GFDA as characterized by (12). However, none of the additional "internal" assumptions of this approach [for example, those listed after (12)] are themselves studied in this paper. Leading corrections to the Green's function approach are discussed in detail in Ref. 12 and these certainly merit study in their own right.

At this point it is useful to realize that the dynamics of the energy-integrated transverse quasielastic strength is also of interest. Thus, in parallel to the longitudinal case, one should also examine the behavior of

$$\begin{aligned}\Sigma_T(|\mathbf{q}|)&=\int_{0^+}^{\infty}R_T(\mathbf{q},\omega)d\omega\ ,\\ S_T(|\mathbf{q}|)&=\int_{0^+}^{|\mathbf{q}|}R_T(\mathbf{q},\omega)d\omega\ ,\end{aligned} \tag{14}$$

under variations in the underlying theoretical assumptions. Although there is no simple transverse analog of the NCSR limit Z, and the enhanced role of meson exchange currents for the transverse response must be borne in mind, (1) and (2) in (14) yield for the TSR

$$\Sigma_T(|\mathbf{q}|)=\sum_{k=1,2}[\langle i|\hat{J}^k(q)^\dagger\hat{J}^k(q)|i\rangle-|\langle i|\hat{J}^k(q)|i\rangle|^2]\ . \tag{15}$$

Application of the Green's function approach to $\Sigma_T(|\mathbf{q}|)$ and $S_T(|\mathbf{q}|)$ parallels that already described for the longitudinal case.

The numerical results of Secs. III–V were obtained using (6c) together with a variety of approximate theoretical and phenomenological optical potentials. Of course, the exact formal optical potential of (6) is far beyond current analytical methods. Because the approximate optical potentials employed certainly do not precisely share the analytical properties of the true optical potential, it is necessary to consider to what degree numerical results based on (6c) actually preserve the NCSR in the appropriate limit. To examine this question consider the CSR in (8) with W^{00} obtained from (6c) using some generic optical potential, $g_{\rm opt}$. In the limit that $g_{\rm opt}$ becomes either the free one-body Green's function g_0, or a one-body Green's function based on a Hermitian potential, then (6c) in (8) yields

$$\lim_{|\mathbf{q}|\to\infty}\Sigma_L^{\rm opt}(|\mathbf{q}|)=\sum_{i_{(1)}}\langle i_{(1)}|\hat{J}^0_{(1)}(q)^\dagger\hat{J}^0_{(1)}(q)|i_{(1)}\rangle\ , \tag{16}$$

where for the Hermitian potential case any bound-state contribution has been restored, including that of the ground state. The absence of a correlation term in (16) is due to the fact that we have ignored any ground state or

Pauli correlations. The important aspect of this limit is that the combination of $\mathrm{Im}(g_{\mathrm{opt}})$ and the inclusion of any bound states is tailored to yield the one-body completeness relation,

$$\sum_n |\chi_n\rangle\langle\chi_n| = 1 , \tag{17}$$

thus maintaining for study a one-body analog of the NCSR. In the case of a non-Hermitian and/or energy-dependent potential, ignoring for now discrete state contributions (for example, unphysical bound states in the continuum),

$$\frac{-1}{\pi}\int \mathrm{Im} g_{\mathrm{opt}} \neq 1 , \tag{18}$$

due to the approximate nature of available optical potentials, so that a spectral analysis of (6c) does not result in the completeness relation and as a consequence one does not precisely obtain the NCSR. This is in contradiction to the case for the exact G_{opt}.

Thus arbitrary g_{opt} will generally not be fully consistent with the NCSR. In high-$|\mathbf{q}|$ studies of sum rule saturation based on (6c) one can dispense with any discrete state complications by requiring that realistic optical potentials produce no discrete eigenvalues. Whether h_{opt} is energy dependent or not, the practical significance of (18) then remains an issue and we must appeal to a reasonable consistency between g_{opt} and G_{opt}. In the limiting cases studied in this paper where the calculations should unambiguously yield the NCSR limit Z but for the presence of non-Hermitian and/or energy-dependent effects, we find that the sum rule is saturated to within 5–10 %. This is in agreement with the scale found in Ref. 38. Since the NCSR defect is small and the contribution of the tail of the quasielastic distribution remains uncertain, the optical theory GFDA is more than adequate for the investigations of the CSR reported in this paper. Although use of a Hermitian energy-independent potential would avoid the above ambiguity, it would do so at the expense of misplaced spectral strength, an unacceptable omission of physically essential many-body final-state dynamics, and would substitute pure phenomenology in place of conceptually clear physical theory.

Finally, it is important to emphasize the relativistic Hilbert-space effect embedded in the relativistic extension of (6c). This effect is most simply seen in the limit where $G_{\mathrm{opt}} \to g_0$, the relativistic version of the free Green's function, $g_0 = (\not{p} - m)^{-1}$. In going to this limit the Dirac optical potential is set to zero, and we want to examine (6c) in the limit of no virtual pair effects (because these only serve to further complicate the sum rule). Thus g_0 is restricted to its positive-energy plane-wave spectrum. In this limit, for low $|\mathbf{q}|$, the nonrelativistic version of (6c) is obtained by restricting the $|i_{(1)}\rangle$ to have Fourier components only in the positive-energy Dirac space and reducing the Dirac matrix elements (Dirac operators and wave functions) to the form of a Pauli matrix element.[51] This requires only a nonrelativistic expansion of the resultant Pauli current operator in powers of $|\mathbf{p}|/m$ and assumes that $|\mathbf{q}|$ is small on the scale of m as well. At this point a considerable inconsistency develops, since the NCSR is now obtained by examining the nonrelativistic version of (6c) in the limit that $|\mathbf{q}|$ grows to values large on the scale of m, thus contradicting the nonrelativistic nature of the development. If one avoids the nonrelativistic reduction and directly evaluates the relativistic plane-wave version of (6c) as $|\mathbf{q}|$ goes asymptotic, instead of $\Sigma_L(|\mathbf{q}|) \to Z$ one finds $\Sigma_L(|\mathbf{q}|) \to Z/2$.[21–23,40] The operational reason for this is the normalization factor $N_D = [(E+m)/2E]^{1/2}$ which appears in the Dirac plane waves: nonrelativistically $N_D^2 \to 1$, whereas relativistically $N_D^2 \to \frac{1}{2}$ (the completeness relation is bilinear in the wave functions so it is N_D^2 which is relevant). The normalization factor cannot be avoided since it is essential to the Dirac completeness relation and it is the fact that the positive-energy Dirac states span only half of the relativistic Hilbert space which is ultimately responsible for the $Z/2$ limit. In view of this result, the NCSR can no longer be characterized as an asymptotic limit in $|\mathbf{q}|$, but must be confined to some limited region in $|\mathbf{q}|$ at best. Alternatively, were it not for the pair effects which further complicate and obscure the issue, one could compensate for N_D^2 effects algebraically. The CSR saturation effects induced by the relativistic phase-space factor are numerically gauged in the next sections.

III. FSI AND RELATIVISTIC EFFECTS

In this section results are presented which elucidate the effects of FSI, relativistic kinematics and Dirac dynamical degrees of freedom on the NCSR. In order to isolate and clearly identify these effects the computational results of this section are obtained using point proton form factors as assumed in the derivation of the ideal NCSR:

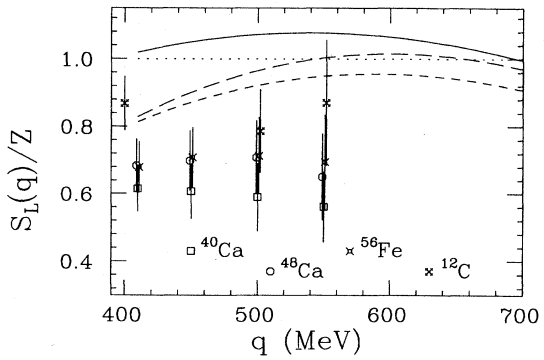

FIG. 1. The Coulomb sum rule curve (integrated longitudinal response) for ^{40}Ca as a function of momentum transfer $|\mathbf{q}|$. Calculations assuming point proton form factors are shown for the nonrelativistic plane-wave approximation (dotted line), the nonrelativistic LDA optical potential from the Bonn N-N interaction (solid line), the nonrelativistic IA optical potential using Franey-Love N-N amplitudes (long-dashed line), and the nonrelativistic optimally factorized IA optical potential using Franey-Love amplitudes (short-dashed line). The data are from Refs. 52–61, where the de Forest prescription is used to remove form-factor effects from the data.

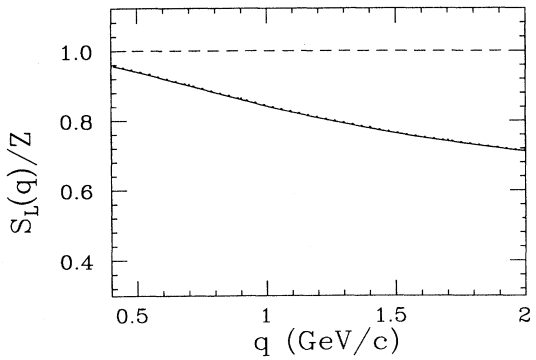

FIG. 2. The CSR curve is displayed for pointlike protons in the nonrelativistic plane-wave (dashed line) and the relativistic plane-wave (solid line) approximations for ^{40}Ca. The dotted line corresponds to a relativistic plane-wave approximation in which only the positive-energy components of the initial bound-state wave functions are included.

$$F_1=\tfrac{1}{2}(1+\tau_3),\quad F_2=0\ . \tag{19}$$

Also shown in Figs. 1–6 is the data for ^{12}C, ^{40}Ca, ^{48}Ca, and ^{56}Fe.[52–61] For the sake of direct comparisons finite form-factor effects are approximately removed from the displayed "data" using a prescription due to de Forest[21] which is described in Sec. V. In addition, there are some important inadequacies in the available data set which must be pointed out. The CSR values and the total experimental integrated responses are obtained by integrating the available data, ignoring strength in the higher-energy tail region where there is presently no data. Hence the CSR integrals are effectively evaluated for $\omega=0^+\rightarrow\approx\frac{2}{3}|\mathbf{q}|$. This implies that the actual, physical CSR values will be somewhat larger than the data pictured. Crude estimates of the amount of strength missing from the data can be made by taking our calculations and integrating in ω from $\frac{2}{3}|\mathbf{q}|\rightarrow|\mathbf{q}|$ into the high-energy tail region. What is found from our calculations is that the CSR data should be increased by about 10%. Recent estimates,[47] in which the response in the high-energy tail region is assumed to have an ω^{-3} falloff, also find the contribution of the unmeasured region to be about 10%. This should be considered when comparisons are made between the data and theoretical predictions, since we have not "corrected" the data for this missing strength in any of the figures. Another dichotomy between the definition of the NCSR and the experimental data is that the NCSR assumes the integral extends from $\omega=0^+\rightarrow\infty$, whereas physical electron scattering is limited to $\omega<|\mathbf{q}|$. We have estimated the quasielastic strength in the region $\omega=|\mathbf{q}|,\ \infty$ by extrapolating the

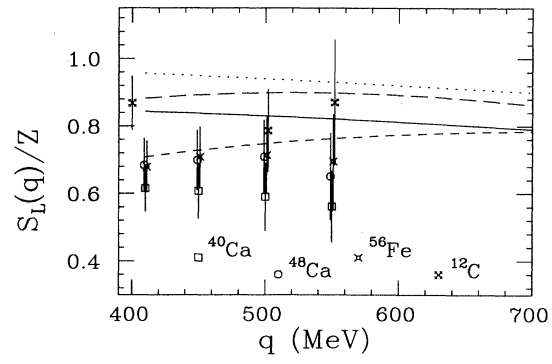

FIG. 3. The CSR curve for ^{40}Ca is shown for several relativistic FSI using point proton form factors. The relativistic plane-wave approximation (dotted line) is shown along with Dirac global phenomenology (solid line), the Dirac IA (short-dashed line), and Dirac Hartree (long-dashed line) FSI calculations.

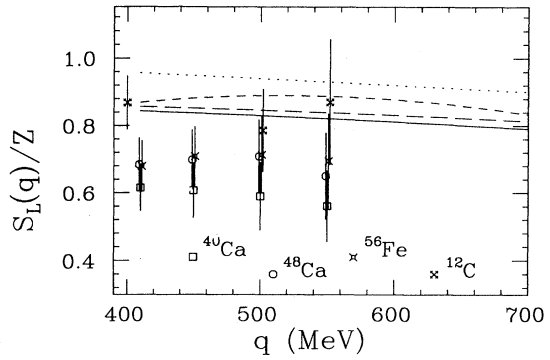

FIG. 4. Point proton CSR ^{40}Ca predictions which isolate various negative-energy contributions using Dirac global phenomenology for the FSI are shown. The full Dirac calculation (solid line), the pure positive-energy NP calculation (short-dashed line), and the NEP calculation with no explicit negative-energy couplings (long-dashed line) are compared, along with the relativistic plane-wave approximation (dotted line) as a reference.

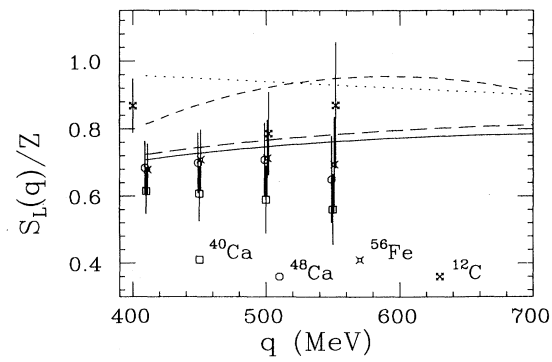

FIG. 5. The same as Fig. 4, except that the calculations employ the optimally factorized Dirac IA optical potential to describe the FSI.

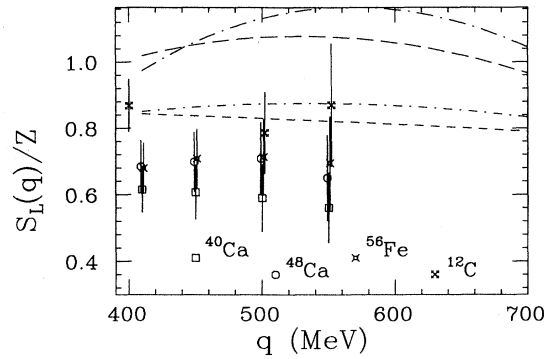

FIG. 6. Predictions for ^{49}Ca using the nonrelativistic LDA with Bonn N-N interactions (long-dashed line) and relativistic Dirac global phenomenological (short-dashed line) FSI are shown. The dashed-dotted curves are predictions obtained using only the real part of the non-Hermitian optical potential in the FSI calculations.

theoretical response curves. It is found that negligible quasielastic strength exists in the physically inaccessible region and any effect on the CSR can be ignored. The error bars in the CSR data are obtained by using the experimental uncertainty in the responses to dictate worst case scenarios. It is assumed that if a least-squares type of approach were used, the error bars in the CSR data would be slightly smaller.

Of the four nuclei for which data is shown, the carbon experimental values are somewhat higher than the rest. One would expect the medium size nuclei to give consistently similar values, but the ^{40}Ca data is significantly and systematically lower than the ^{48}Ca and ^{56}Fe data as is evident in Fig. 1. No obvious theoretical reason for this behavior immediately suggests itself, and this must also be borne in mind when comparisons are made between the data and theoretical predictions.

The GFDA calculations of the CSR are performed using Eq. (13) including FSI, with the integral extending from $\omega=0^+ \rightarrow |\mathbf{q}|$, the physical region. Calculations are made at three discrete values of the momentum transfer, $|\mathbf{q}|=410$, 550, and 700 MeV/c, so that curves shown in the figures are meant to guide the eye. In Figs. 1 and 3–12 plane-wave approximation results are shown as a reference. These correspond to replacing G_{opt} in (6c) with the free noninteracting Green's function g_0 in some particular dynamical limit. All of the theoretical results presented in this paper are for scattering from ^{40}Ca.

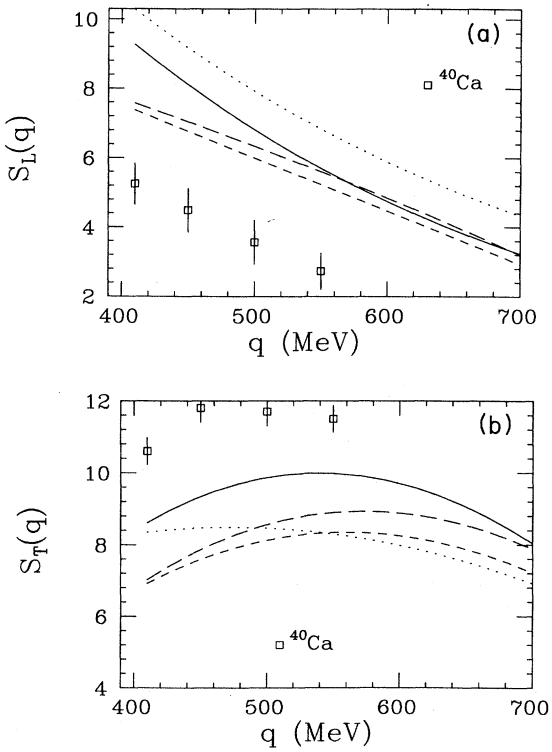

FIG. 7. (a) The same as in Fig. 1, except free electromagnetic form factors are included in the calculation, resulting in the total physical integrated longitudinal response. No attempt is made to remove the form-factor dependence from the calculations or from the data. (b) The same as in (a), except the results are for the integrated transverse response and the relativistic plane-wave result (dotted line) is shown as a reference.

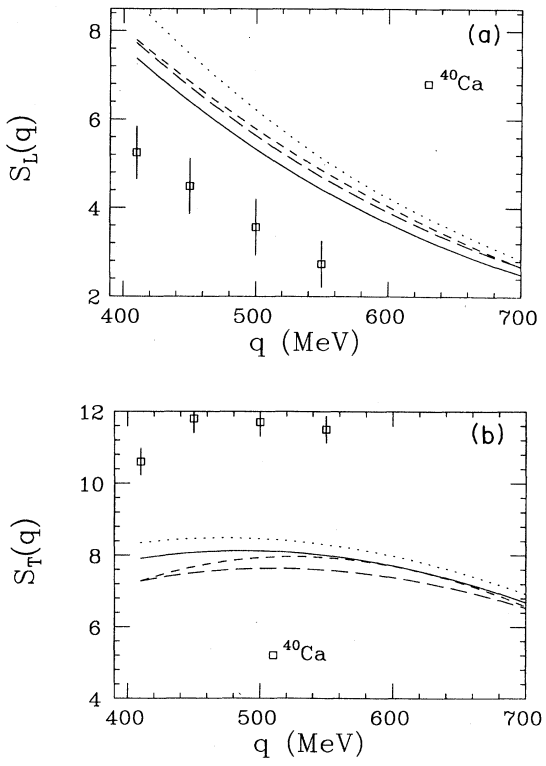

FIG. 8. (a) The same as in Fig. 4 except free electromagnetic form factors are included in the calculation, resulting in the total physical integrated longitudinal response. No attempt is made to remove the form-factor dependence from the calculations or from the data. (b) The same as in (a), except the results are for the integrated transverse response.

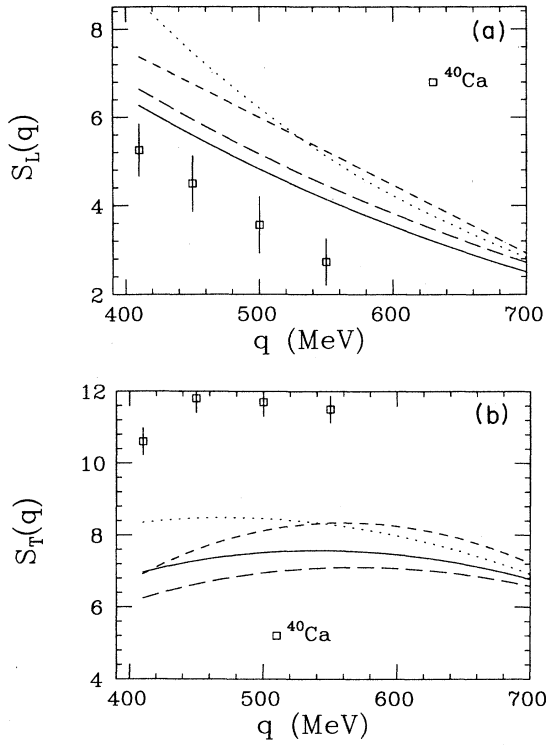

FIG. 9. (a) The same as in Fig. 5 except free electromagnetic form factors are included in the calculation, resulting in the total physical integrated longitudinal response. No attempt is made to remove the form-factor dependence from the calculations or from the data. (b) The same as in (a), except the results are for the integrated transverse response.

A. Nonrelativistic and plane-wave results

In Fig. 1 calculations of the ^{40}Ca integrated longitudinal response for a variety of nonrelativistic FSI are compared. The nonrelativistic plane-wave approximation

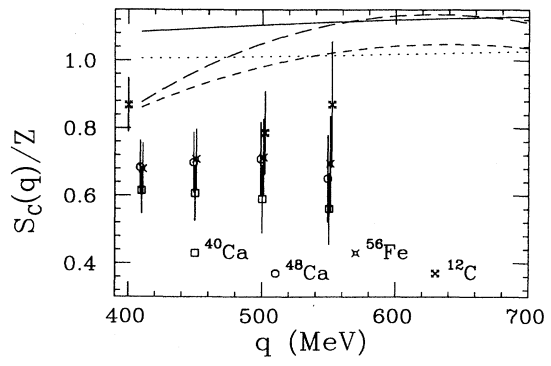

FIG. 10. The same as in Fig. 7(a) except the form-factor dependence and some relativistic effects are approximately removed from the data and the calculations (including the plane-wave case) using the de Forest prescription. The relativistic plane-wave calculation (dotted line) is shown as a reference.

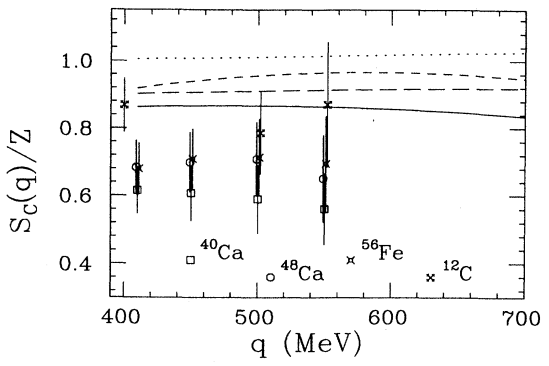

FIG. 11. The same as in Fig. 8(a) except the form-factor dependence and some relativistic effects are approximately removed from the data and the calculations (including the plane-wave case) using the de Forest prescription.

(dotted curve) is shown along with nonrelativistic FSI calculations based on the LDA using a Bonn *N-N* interaction[62–64] (solid curve), the IA with Franey-Love[65] *N-N* amplitudes (long-dashed curve) and the optimally factorized IA (Ref. 66) with Franey-Love *N-N* amplitudes (short-dashed curve) optical potentials. As is expected from the discussion in Sec. II, the plane-wave approximation nicely obeys the NCSR. This is not the case for the various FSI calculations, where nonrelativistic FSI effects on the NCSR are apparent in the figure. The FSI cause the NCSR predictions to be considerably suppressed at lower momentum transfer, modifying the nature of the asymptotic approach to CSR saturation. As $|\mathbf{q}|$ increases to $\gtrsim 500$ MeV/c the theoretical predictions tend to approach the NCSR saturation value. The LDA-Bonn CSR results differ from the IA curves by a non-negligible amount, and this can be traced to differences in the nonhermiticity of the optical potentials used to describe the FSI. The LDA-Bonn optical potential contains local density corrections, which cause a suppression of the strength of the potential in the nuclear interior, thus lead-

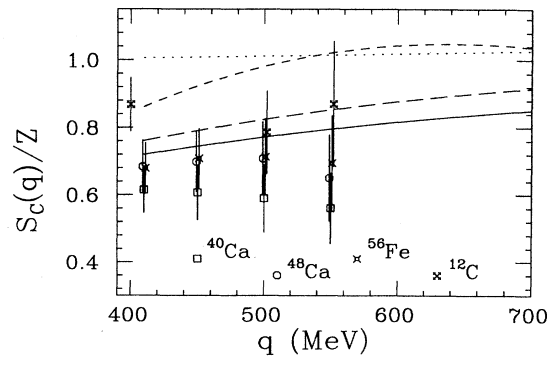

FIG. 12. The same as in Fig. 9(a) except the form-factor dependence and some relativistic effects are approximately removed from the data and the calculations (including the plane-wave case) using the de Forest prescription.

ing to a much smaller imaginary potential. The GFDA is found to be especially sensitive to the non-Hermitian character of the optical potential used. In general a large imaginary potential causes a relative suppression of the CSR integral at lower $|\mathbf{q}|$ shifting strength to higher $|\mathbf{q}|$.[12] In Fig. 1 the solid curve corresponds to an optical potential with a much smaller imaginary part than is the case for the two IA calculations.

A curious effect takes place in Fig. 1 near $|\mathbf{q}| \approx 600$ MeV/c in that the nonrelativistic FSI predictions turn over and begin to decrease away from the NCSR asymptotic limit of 1. The reason for this behavior can be traced to the "nonrelativistic" reduction performed in our calculation of nonrelativistic FSI. Instead of using nonrelativistic wave functions with the nonrelativistic form of the electromagnetic current operator (as is done for the nonrelativistic plane-wave result shown), our nonrelativistic FSI predictions are obtained by taking our relativistic framework and reducing it to the positive-energy sector, implicitly recovering an approximate two component Pauli-like current operator and wave function.[12,45,51] The positive-energy sector of the bound-state and ejectile wave functions are projected out and decomposed into a Pauli wave function times a Pauli-Dirac conversion matrix.[12,45,51] These matrices sandwiching the Dirac current operator produce an equivalent Pauli or "nonrelativistic" current operator. Unlike Eq. (19) this transformation includes relativistic corrections due to Darwin-like terms. In particular, no $|\mathbf{p}|/m$ or small $|\mathbf{p}|$ reduction is performed, and the Dirac normalization factors $N_D = [(E+m)/2E]^{1/2}$ are maintained in the relativistic form. Because of this, the Dirac Hilbert-space effects mentioned earlier are not removed from our nonrelativistic FSI calculations. The importance of this N_D factor is seen in the discussion of Fig. 2, where effects due to N_D arise at larger values of $|\mathbf{q}|$. Hence, the effect clearly seen beyond about $|\mathbf{q}| = 600$ MeV/c is due to relativistic Hilbert-space contributions.

The nonrelativistic plane-wave approximation (dashed curve) is compared to a relativistic plane-wave approximation (solid curve) in Fig. 2. As described earlier, the relativistic plane-wave approximation contains a normalization factor $N_D^2 = (E_k + m)/2E_k$, where in the nonrelativistic limit $N_D^2 \to 1$, but in the relativistic limit $N_D^2 \to \frac{1}{2}$. This factor reflects the fact that the sum over final states in the relativistic case only spans the positive-energy sector of the Hilbert space. In fact, the solid curve in Fig. 2 can be seen to be asymptotically approaching $\frac{1}{2}$. The implication of this is that there are at least two types of conflicting behavior one must consider for the CSR. In the purely nonrelativistic case as $|\mathbf{q}|$ becomes large, the NCSR limit must be approached. However, to the contrary, as $|\mathbf{q}|$ becomes large relativistic effects must be included, thus causing the CSR predictions to asymptotically approach $\frac{1}{2}$ (on the basis of the phase-space factor alone). This phase-space effect, graphically illustrated in Fig. 2, is responsible for the downward trend seen in Fig. 1 for larger $|\mathbf{q}|$. Because the data shown in Fig. 1 are compensated to negate this effect (see Sec. V), while the nonrelativistic FSI calculations are not, one must take account of Fig. 2 when making a precise comparison of data and theory in Fig. 1. This increases the disagreement between purely nonrelativistic theory and experiment. For example, on the basis of Fig. 2 one can obtain approximately the purely nonrelativistic limit of the results shown in Fig. 1 by raising the predictions at $|\mathbf{q}| = 500$ MeV/c and $|\mathbf{q}| = 700$ MeV/c by about 5 and 10%, respectively. Our results for the relativistic phase-space effect are consistent with those reported in Ref. 22.

Also making use of the renormalizations implied by Fig. 2, one sees that the purely nonrelativistic limits of the FSI predictions shown in Fig. 1 are very flat beyond about $|\mathbf{q}| = 600$ MeV/c, and are very nearly converged. Thus it seems that realistic, purely nonrelativistic FSI yield sum rule convergence beyond about 600 MeV/c. As detailed earlier, the formally exact optical potential has the appropriate analytic behavior necessary to recover the spectral completeness relation (17), which practical optical potentials can be expected not to automatically reproduce. Because the NCSR is essentially derived from the completeness relation and because the nonrelativistic FSI employed in the calculations do not perfectly mimic the correct unitary character, the results for nonzero FSI do not uniformly tend to the NCSR limit of unity. This is a defect of optical-potential theory and the associated models and not of the calculations. At the present time it is a defect which must be accepted as the price of dealing with a physically acceptable theory of many-body FSI. The spread of CSR results at $|\mathbf{q}| = 700$ MeV/c is about 10%, consistent with the scale of analytic effects described near the end of Sec. II, although the convergence of all three FSI predictions at 700 MeV/c may also not yet be complete. On the basis of Figs. 1 and 2, the optimally factorized IA optical potential yields CSR predictions which tend nicely to unity and thus appears to have a better analytic character than do the other two nonrelativistic optical potentials, as might be expected on the basis of off-shell unitarity considerations.[66]

An issue to be addressed is at what point, if any, the NCSR can be expected to be obeyed. Solely on the basis of the theoretical predictions of Fig. 1, FSI and relativistic Hilbert-space effects do not allow us to unambiguously choose such a point. The nonrelativistic FSI predictions do appear to reach an extremum near $|\mathbf{q}| \gtrsim 550$ MeV/c, which is approximately twice the Fermi momentum for ^{40}Ca. This same limit has also been suggested by others,[23] but at this momentum transfer $|\mathbf{q}|/m$ is no longer negligible and relativistic effects must surely be considered. At this point, however, there does appear to be a small region ($550 \lesssim |\mathbf{q}| \lesssim 650$ MeV/c) in which the NCSR limit is obeyed in a very rough sense. However, from the combined results of Figs. 1 and 2, the region $|\mathbf{q}| \gtrsim 600$ MeV/c seems to lie within the domain of the NCSR, so long as the experimental data can be compensated for the relativistic phase-space effect in the same spirit as was done for the predictions of Fig. 1 above. Of course, it remains to be seen what the full effects of relativistic FSI dynamics really are. This is detailed in the next subsection. Finally, the dotted curve in Fig. 2, which is essentially indistinguishable from the solid

curve, represents a relativistic plane-wave approximation in which the negative-energy components of the initial Dirac bound-state wave functions are neglected. As is apparent, the effects of such negative-energy components in the initial-state wave functions are extremely small and are completely negligible, and this is true in general; no further distinction between relativistic initial-state wave functions is made in this paper.

B. Relativistic dynamical and non-Hermitian effects

Relativistic FSI calculations are shown in Fig. 3, where Dirac global phenomenology[67,68] (solid curve), Dirac IA (Ref. 49) (short-dashed curve), and Dirac Hartree[69] (long-dashed curve) potentials are used. In comparing these curves with the relativistic plane-wave approximation (dotted curve), it is evident that relativistic FSI suppress the CSR predictions toward the data. (Again, we remind the reader that the relativistic phase-space effect is compensated for in the data shown, but not in the theoretical results, as is evident from the behavior of the relativistic plane-wave result. The same is true of Figs. 4–6.) Also apparent in Fig. 3 is the fact that at $|\mathbf{q}| \approx 700$ MeV/c all three FSI calculations are beginning to parallel the relativistic plane-wave calculation. This suggests that except for the relativistic phase-space effect all three curves have reached "saturation" and are essentially horizontal. However, the three FSI curves are all distinct from the relativistic plane-wave calculation so that, even if the relativistic phase-space effect were to be removed, none of the FSI calculations would saturate at the NCSR value of unity.

The two non-Hermitian calculations shown in Fig. 3, global phenomenology and the Dirac IA, appear to converge to a common value at about $|\mathbf{q}| = 700$ MeV/c, while the Hermitian Hartree calculation is much closer to the relativistic plane-wave result. Although the Hartree potential is real and energy independent, it does shift strength to some degree, and we see that the sum rule limit represented by the plane-wave calculation is not precisely reproduced even at 700 Me/c. Such Hermitian calculations represent well-behaved, but physically and conceptually unclear, results from the standpoint of multichannel reaction theory. In parallel to what was already seen in Fig. 1 for the nonrelativistic theory, the global and the Dirac IA results display differences at lower $|\mathbf{q}|$ because of differing strengths of the imaginary part of the optical potential. The global phenomenology has a smaller imaginary part, characteristic of phenomenological optical potentials relative to their IA counterparts.[70] A closer examination of non-Hermitian effects is given later.

The overall effect of relativistic non-Hermitian FSI is to reduce the CSR theoretical predictions at all $|\mathbf{q}|$ shown in Fig. 3. The relativistic predictions significantly deviate from the NCSR, indicating that a more sophisticated interpretation of the sum rule is necessary. An asymptotic character similar to the NCSR is readily apparent in Fig. 3 (beginning at $|\mathbf{q}| \gtrsim 700$ MeV/c) as long as the relativistic phase-space effect is compensated; however, the results tend to converge to a value about 15% below the idealized NCSR limit. The effects of relativistic FSI appear to preclude a region in $|\mathbf{q}|$ for which the unrenormalized NCSR is reasonably applicable, but suggest that for $|\mathbf{q}| \gtrsim 700$ MeV/c there may be a relatively model-independent relativistic sum rule limit.

The physical difference between the nonrelativistic and relativistic FSI calculations presented here arise generally from two sources: (1) differences in the optical potentials in the positive-energy space (which can be considered to be differences in effective nonrelativistic optical potentials[45,49,51]) and (2) the presence in the relativistic case of negative-energy contributions resulting from couplings to the Dirac sea.[12] To better understand how Dirac dynamic degrees of freedom affect the CSR predictions, the next two figures isolated specific negative-energy contributions. Figures 4 and 5 display predictions based on Dirac global phenomenology and a relativistic impulse approximation, respectively. In both figures the short-dashed curves represent calculations where only positive-energy matrix elements are retained in the FSI. This implies both that the current operator in (2) and (6c) couples the ejectile directly into the positive-energy sector of the Hilbert space only, and that the ejectile then only interacts with the residual nucleus through positive-energy intermediate states. In other words, the outgoing ejectile wave function effectively lies wholly in the positive-energy Dirac space and the optical potential which yields this wave function is not allowed to couple to negative-energy intermediate states (Z graphs are precluded). The long-dashed curves labeled "NEP" (no explicit pairs) include a restricted class of negative-energy effects. The NEP calculations differ from the purely positive-energy calculations in that while the current operator is still allowed only to couple the ejectile directly into positive-energy knockout states, the Dirac final-state interactions are permitted to couple to negative-energy intermediate states. These curves thus include the Z-graph-type negative-energy contributions which seem to be important in elastic proton scattering.[49] The solid curves represent full Dirac calculations which also include direct couplings of the current operator to negative-energy components of the final ejectile scattering states.

In Fig. 4 various predictions obtained using the Dirac global phenomenological optical potential are displayed. The purely positive-energy result lies just below the relativistic plane-wave approximation, and differs considerably from the nonrelativistic behaviors seen in Fig. 1. This is to be expected since it is the full phenomenological optical potential which fits elastic scattering data and not just its positive-energy sector, which is what is employed in obtaining the short-dashed curve. Thus part of the difference between the full relativistic predictions of Fig. 4. and the nonrelativistic predictions of Fig. 1 reflect not virtual pair effects but just differences of an essentially nonrelativistic nature in the optical potentials used.[12] This complication is eliminated in the relativistic IA calculations shown in Fig. 5 where the pure positive-energy IA calculation is the same as the optimally factorized nonrelativistic IA calculation by definition.[49] Therefore, comparisons between the relativistic results shown in Fig. 5 and the nonrelativistic results of Fig. 1 are physically

much clearer than for comparisons using the somewhat arbitrary positive-energy Dirac global calculation of Fig. 4. However, from both figures it is clear that as negative-energy contributions are allowed to contribute to the FSI, the CSR predictions are reduced toward the data by a nonnegligible amount. The negative-energy contributions uniformly suppress the CSR predictions so that the theoretical predictions approach the data and this is true for all of the cases we have treated. As can be seen clearly from Fig. 5 the Dirac sea effects are very large, causing a large suppression of the CSR predictions over the whole range of $|\mathbf{q}|$ shown. The main suppression arises from virtual pair effects due to secondary scattering of the ejectile to virtual negative-energy intermediate states as it proceeds though the nucleus. The explicit pair effect, which arises from the current operator coupling directly to the negative-energy component of the ejectile final-state wave function, provides a smaller but non-negligible contribution. Thus the major relativistic effects on the CSR result from the relativistic phase-space factor and from Z-graph-type optical-model contributions.[49] Relativistic effects on the CSR are large.

To explicitly observe the effect of the non-Hermitian character of the optical potential on the predictions made in the context of the GFDA, calculations are presented in Fig. 6 where the full (complex) result is compared to calculations in which only the real part of the optical potential is retained. The short-dashed (long-dashed) curve represents the full Dirac global phenomenology (nonrelativistic LDA-Bonn) result. The dot-dashed curves represent corresponding calculations using only the real parts of the optical potentials. As is apparent from Fig. 6, the imaginary part of the potentials causes the CSR predictions to be appreciably lower for both the relativistic and nonrelativistic cases over the range $|\mathbf{q}| \gtrsim 410$ MeV/c shown. The fact that the long-dashed-dotted curve is so high is interesting, especially since the potential used is real, but energy dependent, so that it has a somewhat unusual analytic structure and also does not obey (17). From this figure it is apparent that the physical content of the non-Hermitian part of the optical potential is essential for realistic theoretical calculations.

IV. FORM FACTORS AND KINEMATICAL CORRECTIONS

This section presents theoretical calculations in which the current operator incorporates physical free-nucleon form factors as taken from Hohler[71] and as modified in Ref. 72. In Figs. 7–9, the total integrated theoretical response is compared directly with the data, where no attempt is made to divide out any relativistic or form-factor dependence in the calculations or in the data. Figures 7(a), 8(a), and 9(a) display the total integrated longitudinal response, while Figs. 7(b), 8(b), and 9(b) show the total integrated transverse response.

Figure 7(a) is the same as Fig. 1 except that free electromagnetic form factors are included in the calculation. As is readily apparent, the form factors cause dramatic changes in the behavior of the integrated response and lead to a very different character than is found when form-factor effects are divided out or when the idealized NCSR is considered.[73] The nonrelativistic FSI calculations tend to converge toward a common value at higher momentum transfer, implying a consistent nonrelativistic FSI result, but this result overestimates the ^{40}Ca data by a large amount, in agreement with the comparisons of Fig. 1. Even considering the uncertainties in the data, the nonrelativistic results are clearly not able to provide a reasonable description of the data.

The nonrelativistic predictions for the total integrated transverse response are depicted in Fig. 7(b). In this case the data is *underestimated* by a very large amount. This is in agreement with what was found in Ref. 12 for the (unintegrated) transverse response, where the GFDA calculations were found to significantly underestimate R_T. The obvious inference is that the transverse quaiselastic data reflects the presence of some (unknown) many-body mechanisms which are not included within the one-body GFDA formalism, that these mechanisms act predominately in the transverse channel and that they account for the transverse discrepancy. This interpretation is supported by recent $(e,e'p)$ data showing anomalous transverse strength in the dip region[74] and also by recent inclusive $(e,e'p)$ data[75] showing unexplained transverse strength above two-particle threshold.[76] Of course, one must keep in mind that the present calculations also neglect transverse contributions from Δ and other exchange currents. For example, including $\Delta-h$ excitations would likely improve comparison of theory and experiment, although it is also known that the $\Delta-h$ mechanism underestimates the Δ-resonance peak.[77]

Figures 8(a) and 9(a) are the same as Figs. 4 and 5, respectively, except for the inclusion of finite form factors. The relativistic FSI results (solid curves) show CSR predictions which are suppressed a great deal more than are the nonrelativistic FSI calculations shown in Fig. 7(a), providing a much more reasonable description of the data, especially at higher $|\mathbf{q}|$. As was found earlier, negative-energy contributions systematically cause the CSR theoretical curves to be suppressed towards the data. However, Figs. 8(a) and 9(a) also indicate a more pronounced role for explicit pair effects than was apparent in Figs. 4 and 5. The full Dirac calculations are much closer to the data than are the nonrelativistic FSI calculations, but the relativistic results still greatly overestimate the ^{40}Ca CSR data.

Predictions for the corresponding transverse sum using relativistic FSI are shown in Figs. 8(b) and 9(b). In Fig. 8(b), where Dirac global phenomenology is used, the negative-energy contributions play an entirely different role than that observed for the longitudinal case. When the negative-energy FSI effects present in the NEP calculation (long-dashed curve) are added to the purely positive-energy NP calculation (short-dashed curve) a significant suppression of S_T occurs. However, when direct coupling to negative-energy states is included to give the full Dirac calculation, the net result (solid curve) is an enhancement of the NEP result, back up to the NP curve. This distinctive behavior of the transverse sum (relative to that observed for the longitudinal case) is in keeping with the trend of the transverse data, which lies

considerably above the theoretical predictions. This same sort of behavior is also found for the IA in Fig. 9(b) where the NEP result is suppressed compared to the physically realistic nonrelativistic NP curve, while the full Dirac calculation is enhanced compared to the NEP result. However, for the IA case the full Dirac transverse calculation remains somewhat suppressed compared to the nonrelativistic IA result, although not to the same degree as was seen for the longitudinal case. The Dirac calculations continue to underestimate the data for the transverse sum, much more so than do the nonrelativistic FSI predictions. All of these observations concerning the relativistic transverse and longitudinal sums shown in Figs. 8 and 9 reflect analogous effects already seen in the corresponding unintegrated quasielastic (e,e') response functions.[12] The question of a missing many-body transverse mechanism remains.

Recently it has been pointed out that ambiguity in the free neutron form factors can cause nonnegligible uncertainties in theoretical predictions of the quasielastic response functions.[22,78] To gauge this effect we have isolated from our calculations the contribution due to direct knockout of a bound neutron. By comparing the quasielastic strength due to neutron knockout with the total CSR predictions, a measure of the sensitivity of the quasielastic predictions to variations in the free neutron form factors can be obtained. The direct neutron knockout contributions to the CSR predictions are displayed in Table I, given as the fraction of the (corresponding) total CSR prediction. For the plane-wave impulse approximation, as $|\mathbf{q}|$ increases from 410 to 700 MeV/c, the fractional neutron contribution to the CSR, or what will be referred to as "neutron fraction," increases markedly from about 1% to over 3%. This is due to the fact that the coupling between the virtual photon and the neutron ejectile states grows with $|\mathbf{q}|$. The pure positive-energy NP results and the NEP calculations which contain no explicit couplings to the negative-energy space tend to mimic closely the neutron fraction observed for the plane-wave approximation. The NP, NEP, and plane-wave-approximation calculations all share the property of incorporating direct coupling of the current operator to positive-energy final states only.

TABLE I. Fraction of $\int R_L d\omega$ due to direct ejection of a neutron from a single-particle bound state.

FSI type	410 MeV/c	550 MeV/c	700 MeV/c
Global phenomenology			
Full Dirac	0.014	0.032	0.065
NEP	0.009	0.019	0.036
NP	0.009	0.019	0.035
DIA–Love-Franey			
Full Dirac	0.015	0.034	0.065
NEP	0.009	0.019	0.036
NP (nonrelativistic IA)	0.009	0.019	0.036
Plane-wave impulse approximations	0.010	0.019	0.033

Larger neutron fractions are found for the full Dirac calculations. Inclusion of explicit pair effects produces a much larger neutron fraction, ranging from increases of 50–80 % over the NEP results; the larger fractions occur as $|\mathbf{q}|$ increases. For the explicit negative-energy channel contributions there is a strong coupling through the anomalous magnetic moment, and neutron and proton contributions are more nearly on par for the magnetic coupling. The importance of this coupling grows with $|\mathbf{q}|$ and we see that as $|\mathbf{q}|$ increases, the neutron fraction also increases.

The neutron fractions shown in Table I are somewhat different from those found in Ref. 22, where long-range correlations are included in nuclear matter but there are no FSI. The neutron fractions given in Table I are larger than those discussed in Ref. 22, suggesting a greater sensitivity to neutron form-factor variations. The relativistic FSI calculations reported here are sensitive to variations in the neutron form factors, especially to F_2. However, the fractions overall are of small magnitude, being no larger than 6.5%, and thus realistic neutron form-factor variations should not have a large effect on the overall response in the range of $|\mathbf{q}|$ of interest here. One expects F_2 to be much better determined than F_1 and effects dependent on the uncertainty in the neutron form factor to be smaller than the calculated neutron fractions. Direct neutron ejection and associated form factor effects merit further investigation.

V. THEORY VERSUS EXPERIMENT

To recover the CSR in a reasonable form from the data and from realistic theoretical calculations it is necessary to use some specific prescription for removing the form-factor dependence and the relativistic phase-space effect. The usual goal is to recover the idealized predictions of the NCSR, where point protons and nonrelativistic dynamics are assumed. Although this is clearly a model-dependent process, it is one that can be done in the same way for both the data and the theoretical calculations. This should reduce the model dependence to a large degree. A specific prescription developed by de Forest,[21] which is motivated by a reduction of the free relativistic single-nucleon electromagnetic current operator to an effective nonrelativistic form, is often used. Some relativistic effects, notably the relativistic phase-space effect, can also be approximately included in this prescription.[40] The result, which redefines the CSR integral, is[21]

$$S_C(|\mathbf{q}|)=\int_{0^+}^{|\mathbf{q}|} d\omega\, R_L(\mathbf{q},\omega)/\mathcal{F}(q^2)\ , \tag{20}$$

where

$$\mathcal{F}(q^2)=\left[\,|G_E^p(q^2)|^2+\frac{N}{Z}|G_E^n(q^2)|^2\right]\left[1-\frac{q^2}{4m_N^2}\right]\Big/\left[1-\frac{q^2}{2m_N^2}\right], \tag{21}$$

and

$$G_E^i(q^2)=F_1^i(q^2)+\frac{q^2}{4m_N^2}F_2^i(q^2), \quad i=\begin{cases}p, & \text{proton}\\ n, & \text{neutron}\end{cases}.$$

As seen shortly, this method does a very good job of removing relativistic form-factor and phase-space effects incorporated in the relativistic plane-wave calculation up to momentum transfers $|\mathbf{q}|\simeq 1$ GeV. The Dirac dynamical degrees of freedom included in the FSI calculations are not compensated by the de Forest prescription, so that FSI and negative-energy channel effects will cause deviations from the idealized NCSR.

The "data" shown in Figs. 1, 3–6, and 10–12 were obtained by integrating the experimental longitudinal response according to (20) using the de Forest prescription (21) to remove the form-factor dependence. It should also be recalled that, since the experimental values of $R_L(|\mathbf{q}|,\omega)$ range only from $0\rightarrow\frac{2}{3}|\mathbf{q}|$, the true physical values of the CSR integral are crudely estimated to be about 10% higher than the data shown in the figures, due solely to unmeasured strength in the high-energy tail region.

In Fig. 10 the nonrelativistic results of Fig. 7(a) are presented with form-factor and relativistic phase-space effects approximately removed according to (21). The three nonrelatistic FSI curves are calculated as discussed after Fig. 1, using free electromagnetic form factors, and the de Forest prescription is then applied. The dotted curve is the relativistic plane-wave calculation treated with the same prescription. In comparing Fig. 1 with Fig. 10 it can be seen that the de Forest prescription removes the characteristic relativistic phase-space effect of Fig. 1 and that the nonrelativistic FSI predictions now asymptote to a value grater than 1. It has been previously noted that the de Forest prescription causes CSR results to asymptote to a value greater than 1 (Ref. 23) and from Fig. 10 this appears to be the case. In fact, the deviation of the optimal factorization curve of Fig. 10 from unity at ~ 700 MeV/c is due to this effect, as can be appreciated from the parallel behavior of the de Forest compensated relativistic plane-wave calculation. This effect does not fully account for the other two curves shown in Fig. 10: the IA curve is not yet converged, but is decreasing toward unity, whereas the LDA curve is growing. The data, which has also been "treated" with the de Forest prescription, is significantly below the nonrelativistic predictions. Even considering the inadequacies associated with the data, the nonrelativistic FSI calculations do not appear reasonably close to the data.

Figures 11 and 12 consist of the same curves as shown in Figs. 8(a) and 9(a), respectively, except that the de Forest prescription has been used to approximately remove some relativistic and form-factor effects. The relativistic plane-wave approximation (dotted curve) is treated very well by the de Forest prescription with the net result almost consistently equal to 1, differing by only about 3% at the highest $|\mathbf{q}|$ shown. In Fig. 11, as negative-energy effects are systematically included in the Dirac global phenomenological predictions, the CSR results are suppressed more and more toward the data. The net suppression of the NCSR by relativistic FSI, after removing relativistic and form-factor effects by the de Forest prescription, is about 20%. The net result of relativistic effects on the comparison of theory and experiment is somewhat larger, $\sim 30\%$ (see Fig. 2), owing to the relativistic phase-space factor. Superficially, and especially after taking into account the needed upward shift of the data by $\sim 10\%$, these Dirac FSI predictions appear to be in reasonable accord with the data. However, in specifically comparing with the ^{40}Ca data, the predictions are off by a non-negligible amount, even given a 10% enhancement of the data.

In Fig. 12 an optimally factorized relativistic IA calculation using Franey-Love N-N amplitudes is used to describe the FSI. In this case the pure positive-energy (short-dashed curve) calculation is, by construction, the equivalent nonrelativistic IA calculation,[49] thus allowing for a more direct physical comparison between the relativistic and nonrelativistic approaches. Of course, a purely nonrelativistic prediction would not need to have the relativistic phase-space effect removed from it as is the case for Fig. 12. The nonrelativistic IA asymptotes to 1 (at least to the degree consistent with the de Forest compensated plane-wave result), while as Dirac sea effects are added the CSR predictions are systematically suppressed. The suppression is larger than that seen in Fig. 11 at lower $|\mathbf{q}|$ bringing the relativistic FSI predictions closer to the ^{40}Ca data, but at $|\mathbf{q}|\simeq 700$ MeV/c the full Dirac FSI predictions of Figs. 11 and 12 are in very good accord. The two relativistic non-Hermitian FSI calculations consistently produce large suppressions relative to both the nonrelativistic FSI and the relativistic plane-wave results at $|\mathbf{q}|\simeq 700$ MeV/c. Because of the reduced model dependence displayed by these suppressions, obtaining higher-$|\mathbf{q}|$ data would help discriminate between the relativistic and nonrelativistic theories. The quasielastic results obtained with relativistic FSI appear to preclude a region in which the NCSR is reasonably valid. The relativistic FSI suppress the CSR for all values of $|\mathbf{q}|$ considered and the CSR integral no longer asymptotes to the ideal limit of 1.

VI. SUMMARY

This paper reports the results of a systematic study of the modifications to the nonrelativistic Coulomb sum rule induced by form factors, kinematical restrictions, relativistic effects, and realistic final-state interactions. FSI are included via a one-body Green's function doorway approach. An assortment of relativistic and nonrelativistic non-Hermitian optical potentials are used to properly describe the FSI. The reactive content incorporated through the non-Hermiticity of the optical model provides a physically realistic description of the FSI and is shown to have important implications for the NCSR. An analogous transverse sum is also defined and examined, and comparisons are made with existing data.

The physical relativistic kinematical restriction on experimental measurements, $|\mathbf{q}|>\omega$, is predicted by theory to be irrelevant to CSR saturation. The practical restriction $\omega\lesssim\frac{2}{3}|\mathbf{q}|$, however, is predicted to cause the observed experimental quasielastic strength to underestimate the

actual strength by about 10%, in agreement with previous estimates. Neutron knockout contributions are found to be at the level of $\sim 6\%$, indicating neutron form-factor ambiguities bounded by this figure.

Form-factor and relativistic phase-space effects are large, but are found theoretically to be amenable to reliable compensation via a prescription due to de Forest. With corrections and caveats for the foregoing effects, the NCSR is predicted to be well obeyed for momentum transfers beyond about 600 MeV/c in the absence of relativistic final-state interactions.

Nonrelativistic FSI dynamics change the character of the approach to saturation, reducing the integrated response at lower $|\mathbf{q}|$, but allowing convergence to the sum rule in the region $|\mathbf{q}| \gtrsim 600$ MeV/c. However, this result is not complete: whereas important relativistic effects have been acknowledged and compensated, relativistic FSI dynamics are not yet taken into account. Incorporation of virtual pair effects, the essential component of relativistic dynamics, compromises the NCSR. Pair effects induce a large suppression over the entire range $|\mathbf{q}| \gtrsim 410$ MeV/c. Such pair effects may only be expected to further increase in importance for $|\mathbf{q}|$ values larger than those explicitly considered here, so that relativistic dynamics appear to preclude any reasonable regime of validity for the (de Forest compensated) NCSR. However, the full Dirac predictions are consistently and significantly below the NCSR limit, thus bringing the theoretical predictions much closer to the data. To further clarify the dynamics and kinematics responsible for the behavior of the integrated longitudinal response as a function of the momentum transfer $|\mathbf{q}|$, higher momentum transfer data (e.g., ^{40}Ca at $|\mathbf{q}| \gtrsim 700$ MeV/c) are needed.

ACKNOWLEDGMENTS

This work is supported in part by the U.S. Department of Energy. One of us (C.R.C.) would like to express his appreciation to the Physics Division, Los Alamos National Laboratory, for its hospitality. This work was performed (C.R.C.) under the auspices of an Associated Western Universities Fellowship.

[1]K. W. McVoy and L. Van Hove, Phys. Rev. **125**, 1034 (1962).
[2]L. S. Celenza, A. Harindranath, and C. M. Shakin, Phys. Rev. C **33**, 1012 (1986).
[3]P. J. Mulders, Nucl. Phys. **A459**, 525 (1986).
[4]I. Sick, Phys. Lett. **157B**, 13 (1985).
[5]G. van der Steenhoven *et al.*, Phys. Rev. Lett. **57**, 182 (1986).
[6]J. V. Noble, Phys. Rev. Lett. **46**, 412 (1981).
[7]M. Traini, Phys. Lett. B **171**, 266 (1986).
[8]T. D. Cohen, J. W. Van Orden, and A. Picklesimer, Phys. Rev. Lett. **59**, 1267 (1987).
[9]P. J. Mulders, Phys. Rev. Lett. **54**, 2560 (1985).
[10]T. de Forest and P. J. Mulders, Phys. Rev. D **35**, 2849 (1987).
[11]P. J. Mulders and A. E. L. Dieperink, Nucl. Phys. **A483**, 461 (1988).
[12]C. R. Chinn, A. Picklesimer, and J. W. Van Orden, Phys. Rev. C **40**, 790 (1989).
[13]G. Do Dang and Nguyen Van Giai, Phys. Rev. C **30**, 731 (1984).
[14]H. Kurasawa and T. Suzuki, Phys. Lett. B **173**, 377 (1986).
[15]K. Wehrberger and F. Beck, Phys. Rev. C **35**, 298 (1987).
[16]K. Wehrberger and F. Beck, Phys. Rev. C **37**, 1148 (1988).
[17]J. R. Shepard, E. Rost, and J. A. McNeil (submitted to Phys. Rev. C).
[18]C. J. Horowitz, Indiana University Report No. IU/NTC 88-4, 1988.
[19]H. Kurasawa and T. Suzuki, Kyoto University Report RIFP-739.
[20]X. Ji, Phys. Rev. C **39**, 1668 (1989).
[21]T. de Forest, Nucl. Phys. **A414**, 347 (1984).
[22]O. Benhar, Nucl. Phys. **A476**, 272 (1988); O. Benhar, E. Pace, and G. Salme, Phys. Lett. B **195**, 13 (1987).
[23]G. Do Dang, M. L'Huillier, N. Van Giai, and J. W. Van Orden, Phys. Rev. C **35**, 1637 (1987).
[24]T. W. Donnelly, E. L. Kronenberg, and J. W. Van Orden, Nucl. Phys. **A494**, 365 (1989).
[25]W. M. Alberico, P. Czerski, M. Ericson, and A. Molinari, Nucl. Phys. **A462**, 269 (1987).
[26]F. A. Brieva and A. Dellafiore, Phys. Rev. C **36**, 899 (1987).
[27]M. Cavinato *et al.*, Nucl. Phys. **A423**, 376 (1984).
[28]G. Co' and S. Krewald, Nucl. Phys. **A433**, 392 (1985).
[29]U. Stroth, R. W. Hasse, and P. Schuck, Phys. Lett. B **171**, 339 (1986).
[30]U. Stroth, R. W. Hasse, and P. Schuck, Nucl. Phys. **A462**, 45 (1987).
[31]W. M. Alberico, M. Ericson, and A. Molinari, Ann. Phys. (N.Y.) **154**, 356 (1984).
[32]G. Co, K. Quader, R. D. Smith, and J. Wambach, Nucl. Phys. **A485**, 61 (1988).
[33]G. Co', K. Quader, and J. Wambach, Proceedings of the Second Workshop on Problems of Theoretical Nuclear Physics, Cortona, Italy, 1987 [University of Illinois Report ILL-(NU)-87-58, 1987].
[34]S. Drozdz, G. Co', J. Wambach, and J. Speth, Phys. Lett. B **185**, 287 (1987).
[35]J. Jaenicke, P. Schuck, and R. W. Hasse, Phys. Lett. B **214**, 1 (1988).
[36]H. Sagawa, P. M. Boucher, B. Castel, and Y. Okuhara, Phys. Lett. B **219**, 10 (1989).
[37]S. Fantoni and V. R. Pandharipande, Nucl. Phys. **A473**, 234 (1987).
[38]Y. Horikawa, F. Lenz, and N. C. Mukhopadhyay, Phys. Rev. C **22**, 1680 (1980).
[39]A. Dellafiore, F. Lenz, and F. A. Brieva, Phys. Rev. C **31**, 1088 (1985).
[40]J. L. Friar, Ann. Phys. (N.Y.) **81**, 332 (1973).
[41]H. W. L. Naus and J. H. Koch, Phys. Rev. C **36**, 2459 (1987).
[42]A. Fabrocini and F. Fantoni, University of Pisa Report IFUP-2H36/88, 1988.
[43]J. D. Walecka, Ann. Phys. (N.Y.) **83**, 491 (1974).
[44]R. J. Furnstahl, R. J. Perry, and B. D. Serot, Phys. Rev. C **40**, 321 (1989).
[45]A. Picklesimer and J. W. Van Orden, Phys. Rev. C **40**, 290 (1989).
[46]F. Dellagiacoma, R. Ferrari, G. Orlandini, and M. Traini, Phys. Rev. C **29**, 777 (1984).
[47]G. Orlandini and M. Traini, Phys. Rev. C **31**, 280 (1985); **32**,

320 (1985).
[48]H. Feshbach, Ann. Phys. (N.Y.) **19**, 287 (1962).
[49]M. V. Hynes, A. Picklesimer, P. C. Tandy, and R. M. Thaler, Phys. Rev. C **31**, 1438 (1985).
[50]Some additional qualifications concerning minor approximations are need to make this statement precisely true, see later discussion and Ref. 12 for details.
[51]A. Picklesimer, J. W. Van Orden, and S. J. Wallace, Phys. Rev. C **32**, 1312 (1985).
[52]R. Altemus *et al.*, Phys. Rev. Lett. **44**, 965 (1980).
[53]P. Barreau *et al.*, Nucl. Phys. **A358**, 287c (1981).
[54]P. Barreau *et al.*, Nucl. Phys. **A402**, 515 (1983).
[55]C. C. Blatchley *et al.*, Phys. Rev. C **34**, 1243 (1986).
[56]M. Deady *et al.*, Phys. Rev. C **28**, 631 (1983).
[57]M. Deady *et al.*, Phys. Rev. C **33**, 1897 (1986).
[58]B. Frois, Nucl. Phys. **A434**, 57 (1985).
[59]A. Hotta *et al.*, Phys. Rev. C **30**, 87 (1984).
[60]Z. E. Meziani *et al.*, Phys. Rev. Lett. **52**, 2130 (1984).
[61]Z. E. Meziani *et al.*, Phys. Rev. Lett. **54**, 1233 (1985); Z. E. Meziani, Nucl. Phys. **A446**, 113c (1985).
[62]J. J. Kelly, in *Relations Between Structure and Reactions in Nuclear Physics,* edited by D. H. Feng, M. Vallieres, and B. H. Wildenthal (World Scientific, Singapore, 1987), p. 222.
[63]J. J. Kelly *et al.*, Phys. Rev. C **39**, 1222 (1989).
[64]K. Nakayama and W. G. Love, Phys. Rev. C **38**, 51 (1988).
[65]M. A. Franey and W. G. Love, Phys. Rev. C **31**, 488 (1985).
[66]A. Picklesimer, P. C. Tandy, R. M. Thaler, and D. H. Wolfe, Phys. Rev. C **29**, 1582 (1984); **30**, 1861 (1984).
[67]R. H. McCamis *et al.*, Phys. Rev. C **33**, 1624 (1986).
[68]E. D. Cooper, B. C. Clark, S. Hama, and R. L. Mercer, Phys. Lett. B **206**, 588 (1988); **220**, 658e (1989).
[69]C. J. Horowitz and B. D. Serot, Nucl. Phys. **A368**, 503 (1981).
[70]See, for example, P. Schwandt, F. Petrovich, and A. Picklesimer, Indiana University Cyclotron Facility Technical and Scientific Report, 1978, p. 27.
[71]G. Hohler *et al.* Nucl. Phys. **B114**, 505 (1976).
[72]J. L. Firar (private communication).
[73]J. D. Walecka, Nucl. Phys. **A399**, 387 (1983).
[74]R. W. Lourie *et al.*, Phys. Rev. Lett. **56**, 2364 (1986); **57**, 653e (1986).
[75]P. E. Ulmer *et al.*, Phys. Rev. Lett. **59**, 2259 (1987).
[76]T. Takaki, Phys. Rev. C **39**, 359 (1989); Phys. Rev. Lett. **62**, 395 (1989).
[77]J. H. Koch and N. Ohtsuka, Nucl. Phys. **A435**, 765 (1985).
[78]M. Gari and W. Krumpelmann, Phys. Lett. B **173**, 10 (1986).